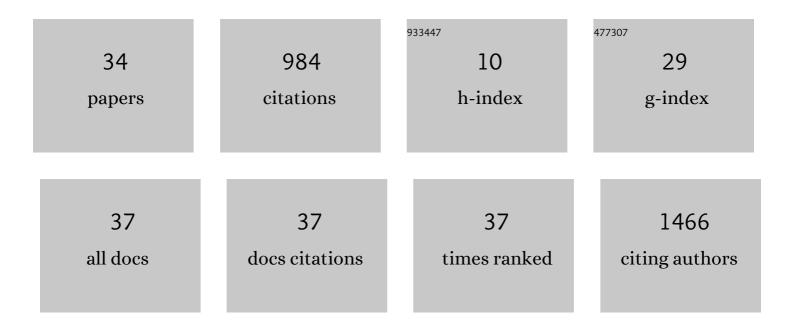


List of Publications by Year in descending order

Source: https://exaly.com/author-pdf/6660781/publications.pdf Version: 2024-02-01



*Ν*Γι Υιι

#	Article	IF	CITATIONS
1	Impact of Boron Doping Concentration on Tunnel Oxide Passivated Contact in Front Surface for N-Type Poly-Si Based Passivated Contact Bifacial Solar Cells. IEEE Journal of Photovoltaics, 2022, 12, 669-677.	2.5	1
2	Improved interface passivation by optimizing a polysilicon film under different hydrogen dilution in N-type TOPCon silicon solar cells. RSC Advances, 2022, 12, 12753-12759.	3.6	0
3	Kirigamiâ€Based Flexible, Highâ€Performance Piezoelectric/Triboelectric Hybrid Nanogenerator for Mechanical Energy Harvesting and Multifunctional Selfâ€Powered Sensing. Energy Technology, 2022, 10,	3.8	6
4	Solar-heating thermocatalytic H ₂ production from formic acid by a MoS ₂ -graphene-nickel foam composite. Green Chemistry, 2021, 23, 7630-7634.	9.0	7
5	Defect Control for Highâ€Efficiency Cu ₂ ZnSn(S,Se) ₄ Solar Cells by Atomic Layer Deposition of Al ₂ O ₃ on Precursor Film. Solar Rrl, 2021, 5, 2100181.	5.8	21
6	Above 15% Efficient Directly Sputtered CIGS Solar Cells Enabled by a Modified Back-Contact Interface. ACS Applied Materials & Interfaces, 2021, 13, 49414-49422.	8.0	8
7	Nâ€Type Surface Design for pâ€Type CZTSSe Thin Film to Attain High Efficiency. Advanced Materials, 2021, 33, e2104330.	21.0	49
8	In Situ Passivation on Rear Perovskite Interface for Efficient and Stable Perovskite Solar Cells. ACS Applied Materials & Interfaces, 2020, 12, 7690-7700.	8.0	12
9	Ferromagnetic anisotropy in scandium-doped AlN hierarchical nanostructures. Journal of Materials Science, 2020, 55, 8325-8336.	3.7	8
10	Wide-spectrum manipulation of triboelectrification-induced electroluminescence by long afterglow phosphors in elastomeric zinc sulfide composites. Journal of Materials Chemistry C, 2019, 7, 4567-4572.	5.5	15
11	9.2%-efficient core-shell structured antimony selenide nanorod array solar cells. Nature Communications, 2019, 10, 125.	12.8	418
12	A vertically layered MoS ₂ /Si heterojunction for an ultrahigh and ultrafast photoresponse photodetector. Journal of Materials Chemistry C, 2018, 6, 3233-3239.	5.5	132
13	Influence of Ce Incorporation from GeSe2 Vapor on the Properties of Cu2ZnSn(S,Se)4 Material and Solar Cells. Coatings, 2018, 8, 304.	2.6	6
14	Microstructural and Optoelectronic Properties of SiGe:H Films at the Transition Edge Fabricated by PECVD. Crystal Research and Technology, 2018, 53, 1700141.	1.3	1
15	Silicon/Organic Hybrid Solar Cells with 16.2% Efficiency and Improved Stability by Formation of Conformal Heterojunction Coating and Moistureâ€Resistant Capping Layer. Advanced Materials, 2017, 29, 1606321.	21.0	126
16	Large Lateral Photovoltage Observed in MoS ₂ Thickness-Modulated ITO/MoS ₂ /p-Si Heterojunctions. ACS Applied Materials & Interfaces, 2017, 9, 18377-18387.	8.0	68
17	Enhanced Photovoltaic Performance of the Inverted Planar Perovskite Solar Cells by Using Mixed-Phase Crystalline Perovskite Film with Trace Amounts of PbI ₂ as an Absorption Layer. Journal of Physical Chemistry C, 2017, 121, 22607-22620.	3.1	11
18	Improved hetero-interface passivation by microcrystalline silicon oxide emitter in silicon heterojunction solar cells. Science Bulletin, 2016, 61, 787-793.	9.0	8

Wei Yu

#	Article	IF	CITATIONS
19	Influences of hydrogen dilution on microstructure and optical absorption characteristics of nc-SiO x :H film. Chinese Physics B, 2015, 24, 108102.	1.4	4
20	Effects of annealing ambient on the photoluminescence properties of Si-rich oxide/SiO2 multilayer films containing Si-nanocrystals. Journal of Materials Science, 2014, 49, 1353-1358.	3.7	7
21	Electrical and thermal transport properties of CdO ceramics. Science China: Physics, Mechanics and Astronomy, 2014, 57, 1644-1648.	5.1	10
22	Optical excitation and emission processes of Si-QD/SiO2 multilayer films with different SiO2 layer thicknesses. Applied Physics A: Materials Science and Processing, 2014, 114, 861-866.	2.3	6
23	Enhanced photon-generated carrier extraction from Si nanostructure under additional infrared light irradiation. Applied Physics Letters, 2013, 102, 201101.	3.3	2
24	Synthesis of full-visible-spectrum luminescent silicon nanocrystals and the origin of the luminescence. Applied Physics A: Materials Science and Processing, 2013, 111, 501-507.	2.3	8
25	Photoresponse and carrier transport of protocrystalline silicon multilayer films. Science Bulletin, 2012, 57, 2624-2630.	1.7	4
26	Laser-induced lateral voltage in epitaxial Al-doped ZnO thin films on tilted sapphire. Applied Physics A: Materials Science and Processing, 2011, 103, 1179-1182.	2.3	3
27	Effects of substrate temperature on structural and optical properties of S-doped ZnO films. , 2011, , .		0
28	Raman scattering characteristics of Mn-doped ZnO films. , 2011, , .		0
29	Influence of substrate temperature on growth of a-Si:H films by reactive facing target sputtering deposition. Science China: Physics, Mechanics and Astronomy, 2010, 53, 807-811.	5.1	10
30	Effect of intrinsic vacancies on the ferromagnetism of V-doped ZnO based on first-principles calculation. Physica Status Solidi (B): Basic Research, 2010, 247, 2185-2189.	1.5	4
31	Epitaxial growth and transport properties of Bi2Sr2Co2Oy thin films by metal organic deposition. Applied Physics Letters, 2009, 94, 162108.	3.3	27
32	Persistent Photoconductivity in Undoped n-Type ZnO Thin Films. , 2009, , .		0
33	Structural and Magnetic Properties of N Doped ZnMnO Film. , 2009, , .		0
34	Improvement of the High-Magnetic-Field Critical Current Density of the Ex-Situ Annealed MgB2 Thick Films by Oxygen Doping. Journal of Superconductivity and Novel Magnetism, 2008, 21, 427-430.	1.8	2